HHS Public Access

Author manuscript

Oncogene. Author manuscript; available in PMC 2012 June 15.

Published in final edited form as:

Oncogene. 2011 December 15; 30(50): 4941–4952. doi:10.1038/onc.2011.199.

EPLIN Downregulation Promotes Epithelial-Mesenchymal Transition in Prostate Cancer Cells and Correlates With Clinical Lymph Node Metastasis

Shumin Zhang[1], **Xu Wang**[2], **Adeboye O. Osunkoya**[1,3], **Shareen Iqbal**[1], **Zhuo Chen**[2], **Susan Müller**[3], **Zhengjia Chen**[4], **Sajni Josson**[5], **Ilsa M. Coleman**[6], **Peter S. Nelson**[6], **Yongqiang A. Wang**[7], **Ruoxiang Wang**[5], **Dong M. Shin**[2], **Fray F. Marshall**[1], **Omer Kucuk**[1,2], **Leland W. K. Chung**[5], **Haiyen E. Zhau**[5,§], and **Daqing Wu**[1,§]

[1]Department of Urology and Winship Cancer Institute, Emory University School of Medicine, Atlanta, GA, USA

[2]Department of Hematology and Medical Oncology, Winship Cancer Institute, Emory University School of Medicine, Atlanta, GA, USA

[3]Department of Pathology & Laboratory Medicine, Emory University School of Medicine, Atlanta, GA, USA

[4]Department of Biostatistics and Bioinformatics, Rollins School of Public Health, Emory University, Atlanta, GA, USA

[5]Uro-Oncology Research Program, Cedars-Sinai Medical Center, Los Angeles, CA, USA

[6]Division of Human Biology, Fred Hutchinson Cancer Research Center, University of Washington, Seattle, WA, USA

[7]Ocean NanoTech, LLC, Springdale, AR, USA

Abstract

Epithelial-mesenchymal transition (EMT) is a crucial mechanism for the acquisition of migratory and invasive capabilities by epithelial cancer cells. By conducting quantitative proteomics in experimental models of human prostate cancer (PCa) metastasis, we observed strikingly decreased expression of EPLIN (epithelial protein lost in neoplasm; or LIM domain and actin binding 1, LIMA-1) upon EMT. Biochemical and functional analyses demonstrated that EPLIN is a negative regulator of EMT and invasiveness in PCa cells. EPLIN depletion resulted in the disassembly of adherens junctions, structurally distinct actin remodeling, and activation of β-catenin signaling. Microarray expression analysis identified a subset of putative EPLIN target genes associated with EMT, invasion and metastasis. By immunohistochemistry EPLIN downregulation was also

[§]**Corresponding authors:** Dr. Daqing Wu (dwu2@emory.edu), Department of Urology and Winship Cancer Institute, Emory University School of Medicine, Atlanta, GA, USA; Dr. Haiyen E. Zhau (Haiyen.Zhau@cshs.org), Uro-Oncology Research Program, Cedars-Sinai Medical Center, Los Angeles, CA, USA.

Supplemental Information

Supplemental Information includes Supplemental Materials and Methods, four Supplemental Figures, eight Supplemental Tables and Supplemental References.

demonstrated in lymph node metastases of human solid tumors including PCa, breast cancer, colorectal cancer and squamous cell carcinoma of the head and neck. This study reveals a novel molecular mechanism for converting cancer cells into a highly invasive and malignant form, and has important implications in prognosing and treating metastasis at early stages.

Keywords

EPLIN; epithelial-mesenchymal transition; prostate cancer; lymph node metastasis; cytoskeleton

Introduction

Acquisition of migratory and invasive capabilities by cancer cells at the primary site is the first step in tumor metastasis (Fidler 2003). This process resembles epithelial-to-mesenchymal transition (EMT), a highly conserved cellular program in embryonic development. During EMT, epithelial cells lose polarity and gain motility through downregulation of epithelial markers, disruption of the cadherin/catenin adhesion complex and re-expression of mesenchymal molecules, which are necessary for invasion and metastasis. Although demonstrating this potentially rapid and transient process *in vivo* has been difficult, and data linking this process to tumor progression are limited and controversial, mounting experimental and clinical evidence, however, supports a crucial role for EMT in cancer metastasis. A number of EMT-related factors and pathways, such as Snail, wnt/β-catenin and hedgehog signaling, have been shown to be shared by embryonic development and tumor progression. The EMT concept, therefore, provides valuable insight into molecular and cellular mechanisms controlling metastasis (Thiery et al 2009).

Metastatic cancer cells are characterized by high motility and invasiveness (Yamazaki et al 2005). Efficient migration and invasion require cancer cells to establish and maintain defined morphologic features, often with lost cell polarity. While stabilization of the actin cytoskeleton is important to the maintenance of an epithelial phenotype, dynamic remodeling of the actin network is crucial for invasive cancer cells to leave the primary tumor, invade through the basement membrane, and extravasate to establish metastases at distant organs. However, cell signaling pathways involved in the regulation of cell-cell adhesion and the actin cytoskeleton network in metastatic cancer cells have not been fully elucidated (Machesky and Tang 2009).

EPLIN (epithelial protein lost in neoplasm; or LIM domain and actin binding 1, LIMA-1) was initially identified as an actin-binding protein that was preferentially expressed in human epithelia but frequently lost in cancerous cells (Maul and Chang 1999, Song et al 2002). Two EPLIN isoforms, the 600-residue EPLIN-α and 759-residue EPLIN-β, differ only at the 5’ end, where an alternative RNA processing event extends the reading frame of EPLIN-β by an additional 160 amino acids (aa) (Chen et al 2000, Maul and Chang 1999). EPLIN contains a central located LIM domain that may allow EPLIN to dimerize with itself or associate with other proteins. Both the N- and C-termini of EPLIN bind actin to promote the parallel formation of filamentous actin polymer (F-actin) structures by cross-linking and bundling actin filaments. EPLIN also inhibits the Arp2/3-mediated nucleation of actin

filaments and suppresses F-actin depolymerization (Maul et al 2003). A recent study demonstrated EPLIN as a key molecule linking the cadherin–catenin complex to F-actin (Abe and Takeichi 2008), which may simultaneously stabilize the adhesion belt formed by the adherens junctions and a bundle of cortical actin filaments near the apical surface of epithelial cells (Pokutta and Weis 2007). The direct interaction between EPLIN and α-catenin *via* both the N- and C-terminal regions is indispensable for the formation of apical actin belt. These observations indicate that EPLIN may be critical to the maintenance of epithelial phenotypes. Nonetheless, investigation into the role of EPLIN in tumor progression remains rudimentary. A recent report inversely correlated EPLIN expression with the aggressiveness and clinical outcome of breast cancer (Jiang et al 2008).

By conducting quantitative proteomics using an experimental model of human PCa metastasis, we observed strikingly decreased EPLIN expression upon EMT. Biochemical and functional analyses indicated that EPLIN is a negative regulator of EMT and invasiveness in PCa cells. Importantly, EPLIN downregulation correlated with lymph node metastases in PCa and other solid tumors. These studies reveal a novel role of EPLIN in the regulation of EMT and tumor metastasis.

Results

Quantitative proteomic analysis of protein expression profile in a PCa EMT model

Previously we reported the ARCaP (androgen refractory cancer of the prostate) cell lineage as an experimental model that resembles the classical descriptions of EMT and closely mimics the clinical pathophysiology of PCa metastasis (Xu et al 2006, Zhau et al 2008). The more epithelial $ARCaP_E$ and more mesenchymal $ARCaP_M$ cells are lineage-related, defined as genetically identical, but behaviorally and phenotypically different. $ARCaP_E$ cells display typical cobblestone morphology and have a relatively low bone metastatic propensity (12.5%) after intracardiac injection in immunocompromised mice, whereas $ARCaP_M$ cells have spindle-shaped fibroblastic morphology associated with increased expression of vimentin and reduced expression of epithelial markers. Importantly, the switch in morphology and gene expression in $ARCaP_M$ cells is associated with high metastatic propensity to skeleton (100%) and soft tissues (33% to adrenal gland). We and others reported that EMT in $ARCaP_E$ cells can be induced by soluble growth factors *in vitro* or by direct interaction with mouse skeleton *in situ* (Graham et al 2008, Zhau et al 2008).

To gain an unbiased insight into the molecular mechanisms underlying PCa EMT, we used an internally standardized gel-free quantitative proteomic technique, cleavable Isotope-Coded Affinity Tag (cICAT) analysis using stable isotope tags (^{12}C and ^{13}C), in combination with 2-dimensional liquid chromatography-tandem mass spectrometry (2-D LC-MS/MS) (Khwaja et al 2006, Khwaja et al 2007), to compare protein expression patterns in the total lysates of $ARCaP_E$ and $ARCaP_M$ cells. We identified 343 unique proteins as expressed in both $ARCaP_E$ and $ARCaP_M$ cells when a ProtScore threshold of 1.3 was used (corresponding to > 95% protein confidence) (Table 1A). Among them, 76 proteins showed differential expression between the cell lines that was considered statistically significant with a *p*-value of less than 0.05: 31 proteins were found to be increased (≥1.20 fold) and 45 proteins were found to be downregulated (≤0.85 fold) in $ARCaP_M$ cells (Table 1B). These

proteins had diverse molecular functions, including cell structure and motility, cell communication, DNA binding and gene expression, metabolism, and signal transduction (Figure S1). In agreement with our previous reports (Xu et al 2006, Zhau et al 2008), proteomics validated increased expression of mesenchymal marker (vimentin) and decreased expression of epithelial markers (cytokeratin-8 and -18) in $ARCaP_M$ cells.

EPLIN downregulation is associated with EMT in the experimental models of PCa

Intriguingly, a striking downregulation of EPLIN-β (by 4.5-fold, Table 1B) was observed in $ARCaP_M$ cells. Western blotting (Figure 1A, left panel) and immunocytochemical (Figure 1A, right panel, top) analyses confirmed that both EPLIN-β and -α isoforms were abundantly expressed in $ARCaP_E$ cells and reduced significantly in $ARCaP_M$ cells. Consistently, immunohistochemical (IHC) analysis showed that EPLIN was substantially expressed in $ARCaP_E$ tumor subcutaneously inoculated in athymic nude mice, but significantly reduced in $ARCaP_M$ tumor (Figure 1A, right panel, bottom). These data indicated that EPLIN downregulation correlated with increased *in vivo* metastatic potential in the ARCaP EMT model. Supporting this notion, a similar association between EPLIN expression and invasive phenotypes was observed in other experimental models of PCa and squamous cell carcinoma of the head and neck (SCCHN) (Figure S2). It was interesting to note that the two EPLIN isoforms were differentially expressed in a cell context-dependent manner: EPLIN-α is prevalently presented in SCCHN cells (Figure S2B), whereas EPLIN-β is the major isoform in LNCaP, C4-2 and MCF-7 cells (Figure S3A, S3B). In comparison, EPLIN-α and -β appeared to be equally expressed by ARCaP and PC3 cells (Figures 1A, S3A).

EPLIN depletion promotes EMT and induces the remodeling of the actin cytoskeleton

To investigate the role of EPLIN in the regulation of EMT, $ARCaP_E$ cells were transiently transfected with an EPLIN siRNA that effectively inhibited expression of both EPLIN-β and -α isoforms (Figure 1B, left panel). $ARCaP_E$ cells expressing control siRNA exhibited a cobblestone-like morphology similar to parent $ARCaP_E$ cells, with tight cell-cell contacts in monolayer cultures. EPLIN depletion in $ARCaP_E$ cells led to loss of cell-cell contacts and the emergence of spindle-shaped and mesenchymal-like morphology (Figure 1B, right panel), indicating the occurrence of EMT in these cells.

Previous studies have demonstrated an important function of EPLIN in stabilizing the actin cytoskeleton (Maul et al 2003, Song et al 2002). To investigate whether EPLIN depletion in PCa cells was associated with the reorganization of the actin cytoskeleton, immunofluorescent confocal microscopy was performed (Figures 1C, S4). In $ARCaP_E$ cells expressing control siRNA, EPLIN largely co-localized with actin stress fibers as revealed by phalloidin staining. EPLIN was also associated with circumferential fibers that were characterized by a circular arrangement along the adhesion belt and bundles of actin filaments linked to the plasma membrane. EPLIN siRNA transfection reduced EPLIN that co-localized with the circumferential fibers and induced actin remodeling, which was manifested as the disassembly of cellular stress fibers, a concomitant gain of actin foci and formation of prominent membrane ruffles. These data indicated that upon EPLIN depletion,

PCa cells may undergo active reorganization of the actin cytoskeleton, which could contribute to increased migratory and invasive capabilities (Yilmaz and Christofori 2010).

EPLIN depletion enhances *in vitro* migration and invasion

We further investigated whether the morphological change of $ARCaP_E$ cells was associated with invasive behavior *in vitro*. Indeed, EPLIN depletion significantly increased the migratory capability of $ARCaP_E$ cells in a wound-healing assay (Figure 1D, upper panel). The infiltration of $ARCaP_E$ cells through Matrigel in a modified Boyden chamber was also remarkably increased (by ~ 2-fold) following EPLIN siRNA transfection (Figure 1D, bottom panel). Such effects of EPLIN siRNA transfection were also observed in other PCa (LNCaP, PC3) and human breast cancer (MCF-7) cells (Figure S3B-S3E). These data suggest that EPLIN downregulation could significantly enhance the *in vitro* invasive capabilities in epithelial cancer cells.

EPLIN depletion suppresses E-cadherin, activates β-catenin signaling and enhances chemoresistance

We established eight $ARCaP_E$ sublines that respectively expressed four different 29-mer EPLIN short-hairpin RNAs (shRNAs) (Table S5). These sublines exhibited similar morphological, biochemical and behavior characteristics. One of such $ARCaP_E$ sublines ($ARCaP_E$-shRNA clone #102) expressing a shRNA sequence of 5'-TAATAGACGGCAATGGACCTCACTATCAT-3' was used as the representative. Consistently, $ARCaP_E$-shRNA cells exhibited a typical mesenchymal morphology compared to epithelial-like control cells ($ARCaP_E$-pRS), indicating the occurrence of EMT upon EPLIN depletion (Figure 2A). Biochemical analyses found that EPLIN inhibition led to decreased E-cadherin, increased vimentin, nuclear translocation of β-catenin and activation of TCF reporter (Figure 2B). Confocal microscopy further demonstrated that shRNA expression resulted in downregulation of E-cadherin on plasma membrane, disassembly of adherens junctions and structurally distinct actin remodeling in PCa cells (Figure 2C). Interestingly, it appeared that EPLIN depletion slightly inhibited proliferation of $ARCaP_E$ cells (Figure 2D), which was associated with an arrested cell cycle progression at the G0/G1 and G2 phases (Figure 2E). On the other hand, however, EPLIN depletion significantly enhanced cell resistance to the treatment of docetaxel and Doxorubicin (by ~8-fold and ~4.4-fold, respectively) (Figure 2F). These results indicated an important role of EPLIN in the regulation of EMT, actin dynamics, proliferation and survival in PCa cells.

EPLIN affects a subset of genes involved in EMT and invasion

To identify genes that are potentially affected by EPLIN, we analyzed the transcriptome of $ARCaP_E$-shRNA cells and control cells. Microarray analysis found that there were 1026 genes significantly upregulated and 828 genes significantly downregulated in $ARCaP_E$-shRNA cells (Figure 3A), which could be categorized into different function clusters (Tables S2 and S3), including those involved in the regulation of EMT, Wnt/β-catenin signaling, actin cytoskeleton, invasion and metastasis, adhesion and extracellular matrix remodeling, and growth factor signaling (Figure 3B; Tables S3 and S4). Several approaches were used to validate the differential expression of selected putative EPLIN target genes. Reverse

transcription-PCR (RT-PCR) assays (Figure 3C, left panel) demonstrated increased expression of versican, matrix metalloproteinase-7 (MMP-7), Bcl-2A, fibroblast growth factor 5 (FGF5), and downregulation of inhibitor of differentiation 2 (ID2), myosin light chain kinase (MYLK), and insulin-like growth factor-binding protein-3 (IGFBP-3) in $ARCaP_E$-shRNA cells. Western blot analyses (Figure 3C, right panel) confirmed downregulation of IGFBP-3 at protein level, and showed that EPLIN depletion increased expression of cAMP-responsive element-binding protein (CREB) and myeloid cell leukemia-1 (Mcl-1) whose upregulation has been associated with clinical PCa metastasis (Wu et al 2007, Zhang et al 2010). EPLIN depletion significantly increased expression of zinc finger E-box-binding homeobox 1 (ZEB1), a potent EMT activator that transcriptionally suppresses E-cadherin expression (Wellner et al 2009), whereas it inhibited Krueppel-like factor (KLF) 5, a zinc finger transcription factor implicated in PCa progression (Dong and Chen 2009). Consistently, increased presence of ZEB1 and reduced expression of KLF5 in the nucleus of $ARCaP_E$-shRNA cells were observed. Expression of Slug and Twist, two master regulators of EMT, was not affected by EPLIN depletion in PCa cells. Zymogram assay (Figure 3D) showed that expression of activated MMP-27 was significantly increased upon EPLIN silencing. EPLIN depletion also resulted in a remarkable increase (~5.6-fold) in the proportion of $ARCaP_E$ cells carrying the $CD44^{high}/CD24^{negative}$ marker profile associated with cancer stem cell (CSC) subpopulation (Klarmann et al 2009) (Figure 3E). Interestingly, EPLIN shRNA suppressed expression of several microRNAs (miRNAs), including miR-205 and two miR-200 family members (miR-200b and miR-429) (Figure 3F), whose downregulation is thought to be the essential feature of EMT and acquisition of CSC properties (Lang et al 2009). These data indicate that EPLIN downregulation may coordinately activate multiple pro-EMT programs in PCa cells.

EPLIN downregulation is associated with lymph node metastasis in PCa, breast cancer, colon cancer and SCCHN

We searched two global cancer transcriptome databases, i.e., the Gene Expression Omnibus (GEO) and ONCOMINE, for the expression pattern of EPLIN in a number of epithelial cancers. Analyses on four independent sets of microarray data on clinical PCa (Chandran et al 2007, Lapointe et al 2004, Varambally et al 2005, Yu et al 2004) revealed that EPLIN transcripts were expressed at a similar level in primary tumors and normal prostatic tissues, but were remarkably reduced in metastatic tumors (Figure 4A). We examined the IHC staining of EPLIN in matched pairs of PCa tissue specimens from primary PCa and lymph node metastases. As shown in Figure 4B, EPLIN expression was significantly reduced in lymph node metastases.

Analyses of the ONCOMINE database found that metastatic colon cancer expresses significantly lower levels of EPLIN transcripts compared to primary tumors (Figure 5A). We examined IHC expression of EPLIN in a human colorectal cancer tissue microarray consisting of matched pairs of primary tumors and lymph node metastases. Figure 5B shows that EPLIN expression was significantly decreased in lymph node metastatic tumors. Similarly, EPLIN immunointensity was markedly reduced in breast cancer lymph node metastases compared to their matched primary tumors (Figure 5C). We finally evaluated IHC expression of EPLIN in 10 pairs of tissue specimens from primary and lymph node

metastatic SCCHN. EPLIN expression was also decreased in lymph node metastases (Figure 5D). Collectively, these observations suggested that EPLIN downregulation may be an indicator of clinical metastasis in PCa and several other epithelial cancers.

Discussion

In this study, a quantitative proteomics characterized a remarkable downregulation of EPLIN upon EMT in an experimental model of PCa metastasis. Biochemical and functional evidence revealed that EPLIN is a negative regulator of EMT and invasiveness in PCa cells. EPLIN downregulation was found to significantly disrupt epithelial structures, induce actin cytoskeleton remodeling, affect specific gene expression profiles and activate a pro-EMT program. Importantly, using human tumor specimens as the “gold standard”, an inverse correlation between EPLIN expression and clinical lymph node metastasis was observed in a variety of solid tumors. These studies elucidate a causal role of EPLIN in EMT and support its new function as a tumor metastasis suppressor (Figure 6).

Emerging proteomic techniques offer robust and unbiased approaches for molecular profiling of the complex metastatic process, including EMT, at the protein level (Varambally et al 2005). However, to date only a limited number of proteomic studies were reported in EMT models of human cancer (Mathias and Simpson 2009). In this report, we utilized a quantitative proteomic approach, i.e., cICAT in combination with 2-D LC-MS/MS, to characterize protein profile in a novel model for PCa EMT and metastasis. A panel of 76 proteins were found to be significantly altered in the epithelial-like and lowinvasive $ARCaP_E$ cells and the mesenchymal-like and highly metastatic $ARCaP_M$ cells. Of those, several have been identified to be associated with EMT and metastasis in previous proteomic studies, including increased expression of vimentin, tropomyosin and heat-shock protein β-1 (HSP-β1), and reduced expression of cytokeratin-8, -18 and 14-3-3ε (Keshamouni et al 2006, Keshamouni et al 2009, Larriba et al 2010, Wei et al 2008, Willipinski-Stapelfeldt et al 2005). We also observed a concurrent upregulation of S100A10 and its annexin A2 ligand in $ARCaP_M$ cells, which is interesting since activation of the S100A10/Annexin A2 signaling has been associated with plasminogen activation and increased tumor invasion and metastasis (Kwon et al 2005, O'Connell et al 2010). These results validated the application of quantitative proteomics in identifying key factors implicated in EMT and the acquisition of invasiveness in PCa cells.

At the cellular levels, EMT is characterized by the disappearance of the apical-basal polarity in epithelial cells. Remodeling of the actin cytoskeleton is a prerequisite for the acquisition of migratory and invasive capabilities during this process (Machesky and Tang 2009, Yamazaki et al 2005, Yilmaz and Christofori 2009). Our proteomic analysis identified a functional group of proteins that have been implicated in the regulation of actin dynamics and cellular structure (Figure S1), which includes 6 proteins upregulated (vimentin, keratin II, tropomysin, profilin 1, HSP-β1, and actin-α) and 8 proteins downregulated (LIMA1 or EPLIN, S100A4, echinoderm microtubule associated protein like 5, lamin A/C, matrin-3, tubulin-β2C, cytokeratin-18 and -8) in $ARCaP_M$ cells. Among them, EPLIN has been demonstrated as an indispensible component of the core cell polarity complexes, linking the cadherin– catenin complex to the actin cytoskeleton and actively stabilizes the actin bundles

(Abe and Takeichi 2008, Maul et al 2003, Song et al 2002). Mechanistic studies in non-cancerous (such as NIH3T3) and cancerous (such as MCF-7) cells indicated that both EPLIN isoforms are capable of suppressing F-actin depolymerization and enhancing the bundling of actin filaments through an Arp2/3-mediated mechanism. Downregulation of EPLIN, therefore, may result in cytoskeletal reorganization due to a loss of stability of mature actin filament structure and facilitated turnover of filaments in epithelial cancer cells. Indeed, as revealed by confocal microscopy, EPLIN depletion in $ARCaP_E$ cells significantly reduced cellular actin stress fibers and promoted the formation of more dynamic actin filament structures such as membrane ruffling, which may contribute to increased motility of PCa cells. Furthermore, we showed that EPLIN depletion in PCa cells could directly facilitate disassembly of the apical adherens junctions-actin machinery and redistribution of the components of the cadherin-catenin complex, thereby substantially perturbing actin dynamics. These structural alterations may promote transition to mesenchymal morphology and enhance the plasticity and migratory capabilities of epithelial cancer cells (Yamazaki et al 2005) (Figure 6).

Accumulating evidence support that actin and actin-associated proteins are indispensible components of the regulatory machinery of eukaryotic gene transcription, for example, involving in the modulation of RNA polymerase II-dependent transcription and facilitating RNA polymerase I transcription and possibly downstream events during ribosomal RNA biogenesis (Percipalle et al 2009, Schneider and Grosschedl 2007). EPLIN dysregulation may have a remarkable influence on the dynamics of cytoskeleton and its interplay with nuclear architecture, thereby regulating global gene expression. In fact, it has been shown that EPLIN is required for the local accumulation of key cytokinesis proteins at the cleavage furrow during ingression, which is critical to cytokinesis and genomic stability. EPLIN depletion in Hela cells results in cytokinesis failure and formation of multinucleation and aneuploidy (Chircop et al 2009). In this study, we identified approximately 1,800 genes that were significantly affected by EPLIN depletion in PCa cells. Among them, some have been implicated in the regulation of EMT and tumor metastasis, for instance, ZEB1 (Schmalhofer et al 2009, Wellner et al 2009), IGFBP-3 (Renehan et al 2004), versican (Sakko et al 2003, Sung et al 2008) and MMPs (Katiyar 2006). Notably, EPLIN depletion in several PCa and breast cancer cells resulted in downregulation of E-cadherin (Figures 2B, S3B), a hallmark of EMT and acquired invasiveness in most solid tumors. These interesting findings suggest that EPLIN dysregulation could profoundly affect gene expression at transcriptional levels, which may be an underlying mechanism for EPLIN regulation of EMT.

Loss of expression or function of tumor metastasis suppressors is requisite for the development of local invasion and distant metastases (Smith and Theodorescu 2009). Previous studies have described several potential metastasis suppressor genes in PCa (Thiolloy and Rinker-Schaeffer 2010, Wong et al 2007). EPLIN was initially identified as an epithelial protein that is abundantly expressed in normal epithelia but significantly downregulated at mRNA level in a limited number of cancerous cells (Maul and Chang 1999). This expression profile suggested that EPLIN may function as a suppressor of tumorigenesis in epithelial cancers. Nonetheless, the role and clinical significance of EPLIN during tumor progression remain largely unknown. Our data presented here demonstrated that EPLIN protein is substantially expressed by most low-invasive epithelial cancer cells

examined, but significantly decreased in those with high invasive capabilities (Figures 1A and S2), implying the involvement of EPLIN in tumor invasion and metastasis. Biochemical and functional analyses further uncovered the function of EPLIN in the maintenance of epithelial phenotypes in low-invasive PCa cells, and a causal role of EPLIN downregulation in promoting EMT and conferring invasiveness, including enhanced migratory and invasive behaviors and resistance to chemotherapy agents. Interestingly, EPLIN depletion resulted in delayed cell cycles and suppressed *in vitro* proliferation, an effect that has been observed when overexpressing certain pro-metastasis genes (such as Snail, Slug) in PCa cells (Emadi Baygi et al 2010, Liu et al 2010, McKeithen et al 2010), suggesting a complicated role of EPLIN in the regulation of PCa cell proliferation and differentiation.

To explore the clinical significance of EPLIN in human cancers, we analyzed the expression profile of EPLIN based on published microarray data. In both PCa and colorectal cancer specimens, EPLIN transcripts were found to be reduced in primary tumors and further decreased in metastatic disease. These observations argue against a simple role of EPLIN as a tumor suppressor, and suggest a new function of EPLIN in late stages of tumor progression in addition to tumorigenesis (Jiang et al 2008, Maul and Chang 1999). Indeed, EPLIN protein could be detected at relatively high levels in primary PCa, breast cancer, colorectal cancer and SCCHN, but was significantly reduced in their matched lymph node metastases. Although the numbers of tissue specimens included in this study are limited due to the extreme difficulty of obtaining paired tumor samples from primary and metastatic human cancers, our data clearly demonstrate that EPLIN downregulation could be an indicator of tumor metastasis in a variety of epithelial cancers.

Materials and Methods

Proteomic Analysis

Quantitative proteomic analysis was performed at Emory University Microchemical and Proteomics Facility. Total proteins from $ARCaP_E$ and $ARCaP_M$ cells were prepared in the absence of proteinase inhibitors by trichloroacetic acid precipitation and resuspended in denaturing buffer. cICAT analysis, in combination with liquid 2-dimensional liquid chromatography-tandem mass spectrometry, was performed as described previously (Khwaja et al 2006, Khwaja et al 2007). Briefly, the $ARCaP_E$ and $ARCaP_M$ samples were separately labeled with light and heavy reagent, mixed in equal total protein ratio, and digested overnight with trypsin. The peptides were then desalted using a strong cation-exchange cartridge, and the cICAT-modified, cysteine-containing peptides were enriched/purified using a monomeric avidin column (Applied Biosystems). The biotin tag was cleaved off by treatment with trifluoroacetic acid and the sample was dried and reconstituted in 10% formic acid. A portion of the sample was analyzed using an Ultimate 3000 nanoHPLC system (Dionex, Sunnyvale, CA) using a Vydac C18 silica column interfaced to a QSTAR XL mass spectrometer (Applied Biosystems, CA). The MS/MS data from each salt cut were combined and processed by ProteinPilot software (Applied Biosystems, Carlsbad, CA) for protein identification and quantification. Only proteins with a ProtScore >1.0 (Confidence Interval >85%) were considered. Proteins were considered differentially

expressed if multiple peptides generated concordant cICAT ratios in both analyses. Proteins were grouped into functional categories using the UniProt Knowledgebase (UniProtKB).

Microarray Analysis

A reference standard RNA for use in two-color oligo arrays was prepared as described previously (Arnold et al 2009). Total RNA from triplicate preparations of control and knockdown samples as well as reference total RNA samples were amplified and hybridized to Agilent 44K whole human genome expression oligonucleotide microarray slides as previously described (Koreckij et al 2009). Spots of poor quality or average intensity levels <300 were removed from further analysis. The Statistical Analysis of Microarray (SAM) program (Tusher et al 2001) was used to analyze expression differences between control and knockdown groups using unpaired, two-sample *t* tests.

Immunohistochemical Analysis

Human PCa tissue specimens were obtained from Emory University Hospital Department of Pathology. Human SCCHN tissue specimens were obtained from the Pathology Core of the Emory University Head and Neck Cancer Specialized Programs of Research Excellence (SPORE). Human colorectal cancer and breast cancer tissue microarrays were purchased from US BioMax, Inc (Rockville, MD). IHC staining of EPLIN was performed as described previously (Wu et al 2007) using a rabbit anti-EPLIN antibody (NB100-2305, Novus Biologicals, LLC, Littleton, CO) at a dilution of 1:50.

Statistical Analysis

Significance levels for comparisons of protein expression in tumor tissue specimens were calculated by using the 2-sample *t* test. Treatment effects were evaluated using a two-sided Student's *t* test. All data represent three or more experiments. Errors are S.E. values of averaged results, and values of $p \leq 0.05$ were taken as a significant difference between means.

Supplementary Material

Refer to Web version on PubMed Central for supplementary material.

Acknowledgements

We thank Dr. Jin-Tang Dong for critical reading of the manuscript, and Dr. Anthea Hammond for editorial assistance. This work was supported by Department of Defense PC060566, American Cancer Society RSG-10-140-01, Georgia Cancer Coalition Cancer Research Award, Kennedy Seed Grant, Emory University Research Committee Award, Winship MPB Seed Grant (D.W), National Cancer Institute grants P01 CA98912, R01 CA122602, and Department of Defense PC060866 (L.W.K. C), Georgia Cancer Coalition Distinguished Scholar Grant (O.K), and National Cancer Institute grant 1R43CA141870 (Y.A. W).

References

Abe K, Takeichi M. EPLIN mediates linkage of the cadherin catenin complex to F-actin and stabilizes the circumferential actin belt. Proc Natl Acad Sci U S A. 2008; 105:13–19. [PubMed: 18093941]

Arnold RS, Sun CQ, Richards JC, Grigoriev G, Coleman IM, Nelson PS, et al. Mitochondrial DNA mutation stimulates prostate cancer growth in bone stromal environment. Prostate. 2009; 69:1–11. [PubMed: 18850577]

Chandran UR, Ma C, Dhir R, Bisceglia M, Lyons-Weiler M, Liang W, et al. Gene expression profiles of prostate cancer reveal involvement of multiple molecular pathways in the metastatic process. BMC Cancer. 2007; 7:64. [PubMed: 17430594]

Chen S, Maul RS, Kim HR, Chang DD. Characterization of the human EPLIN (Epithelial Protein Lost in Neoplasm) gene reveals distinct promoters for the two EPLIN isoforms. Gene. 2000; 248:69–76. [PubMed: 10806352]

Chircop M, Oakes V, Graham ME, Ma MP, Smith CM, Robinson PJ, et al. The actin-binding and bundling protein, EPLIN, is required for cytokinesis. Cell Cycle. 2009; 8:757–764. [PubMed: 19221476]

Dong JT, Chen C. Essential role of KLF5 transcription factor in cell proliferation and differentiation and its implications for human diseases. Cell Mol Life Sci. 2009; 66:2691–2706. [PubMed: 19448973]

Emadi Baygi M, Soheili ZS, Schmitz I, Sameie S, Schulz WA. Snail regulates cell survival and inhibits cellular senescence in human metastatic prostate cancer cell lines. Cell Biol Toxicol. 2010; 26:553–567. [PubMed: 20397042]

Fidler IJ. The pathogenesis of cancer metastasis: the 'seed and soil' hypothesis revisited. Nat Rev Cancer. 2003; 3:453–458. [PubMed: 12778135]

Graham TR, Zhau HE, Odero-Marah VA, Osunkoya AO, Kimbro KS, Tighiouart M, et al. Insulin-like growth factor-I-dependent up-regulation of ZEB1 drives epithelial-to-mesenchymal transition in human prostate cancer cells. Cancer Res. 2008; 68:2479–2488. [PubMed: 18381457]

Jiang WG, Martin TA, Lewis-Russell JM, Douglas-Jones A, Ye L, Mansel RE. Eplin-alpha expression in human breast cancer, the impact on cellular migration and clinical outcome. Mol Cancer. 2008; 7:71. [PubMed: 18796137]

Katiyar SK. Matrix metalloproteinases in cancer metastasis: molecular targets for prostate cancer prevention by green tea polyphenols and grape seed proanthocyanidins. Endocr Metab Immune Disord Drug Targets. 2006; 6:17–24. [PubMed: 16611161]

Keshamouni VG, Michailidis G, Grasso CS, Anthwal S, Strahler JR, Walker A, et al. Differential protein expression profiling by iTRAQ-2DLC-MS/MS of lung cancer cells undergoing epithelial-mesenchymal transition reveals a migratory/invasive phenotype. J Proteome Res. 2006; 5:1143–1154. [PubMed: 16674103]

Keshamouni VG, Jagtap P, Michailidis G, Strahler JR, Kuick R, Reka AK, et al. Temporal quantitative proteomics by iTRAQ 2D-LC-MS/MS and corresponding mRNA expression analysis identify post-transcriptional modulation of actin-cytoskeleton regulators during TGF-beta-Induced epithelial-mesenchymal transition. J Proteome Res. 2009; 8:35–47. [PubMed: 19118450]

Khwaja FW, Svoboda P, Reed M, Pohl J, Pyrzynska B, Van Meir EG. Proteomic identification of the wt-p53-regulated tumor cell secretome. Oncogene. 2006; 25:7650–7661. [PubMed: 17043663]

Khwaja FW, Reed MS, Olson JJ, Schmotzer BJ, Gillespie GY, Guha A, et al. Proteomic identification of biomarkers in the cerebrospinal fluid (CSF) of astrocytoma patients. J Proteome Res. 2007; 6:559–570. [PubMed: 17269713]

Klarmann GJ, Hurt EM, Mathews LA, Zhang X, Duhagon MA, Mistree T, et al. Invasive prostate cancer cells are tumor initiating cells that have a stem cell-like genomic signature. Clin Exp Metastasis. 2009; 26:433–446. [PubMed: 19221883]

Koreckij TD, Trauger RJ, Montgomery RB, Pitts TE, Coleman I, Nguyen H, et al. HE3235 inhibits growth of castration-resistant prostate cancer. Neoplasia. 2009; 11:1216–1225. [PubMed: 19881957]

Kwon M, MacLeod TJ, Zhang Y, Waisman DM. S100A10, annexin A2, and annexin a2 heterotetramer as candidate plasminogen receptors. Front Biosci. 2005; 10:300–325. [PubMed: 15574370]

Lang SH, Frame FM, Collins AT. Prostate cancer stem cells. J Pathol. 2009; 217:299–306. [PubMed: 19040209]

Lapointe J, Li C, Higgins JP, van de Rijn M, Bair E, Montgomery K, et al. Gene expression profiling identifies clinically relevant subtypes of prostate cancer. Proc Natl Acad Sci U S A. 2004; 101:811–816. [PubMed: 14711987]

Larriba MJ, Casado-Vela J, Pendas-Franco N, Pena R, Garcia de Herreros A, Berciano MT, et al. Novel snail1 target proteins in human colon cancer identified by proteomic analysis. PLoS One. 2010; 5:e10221. [PubMed: 20421926]

Liu J, Uygur B, Zhang Z, Shao L, Romero D, Vary C, et al. Slug inhibits proliferation of human prostate cancer cells via downregulation of cyclin D1 expression. Prostate. 2010

Machesky LM, Tang HR. Actin-based protrusions: promoters or inhibitors of cancer invasion? Cancer Cell. 2009; 16:5–7. [PubMed: 19573806]

Mathias RA, Simpson RJ. Towards understanding epithelial-mesenchymal transition: a proteomics perspective. Biochim Biophys Acta. 2009; 1794:1325–1331. [PubMed: 19439204]

Maul RS, Chang DD. EPLIN, epithelial protein lost in neoplasm. Oncogene. 1999; 18:7838–7841. [PubMed: 10618726]

Maul RS, Song Y, Amann KJ, Gerbin SC, Pollard TD, Chang DD. EPLIN regulates actin dynamics by cross-linking and stabilizing filaments. J Cell Biol. 2003; 160:399–407. [PubMed: 12566430]

McKeithen D, Graham T, Chung LW, Odero-Marah V. Snail transcription factor regulates neuroendocrine differentiation in LNCaP prostate cancer cells. Prostate. 2010; 70:982–992. [PubMed: 20166136]

O'Connell PA, Surette AP, Liwski RS, Svenningsson P, Waisman DM. S100A10 regulates plasminogen-dependent macrophage invasion. Blood. 2010; 116:1136–1146. [PubMed: 20424186]

Percipalle P, Raju CS, Fukuda N. Actin-associated hnRNP proteins as transacting factors in the control of mRNA transport and localization. RNA Biol. 2009; 6

Pokutta S, Weis WI. Structure and mechanism of cadherins and catenins in cell-cell contacts. Annu Rev Cell Dev Biol. 2007; 23:237–261. [PubMed: 17539752]

Renehan AG, Zwahlen M, Minder C, O'Dwyer ST, Shalet SM, Egger M. Insulin-like growth factor (IGF)-I, IGF binding protein-3, and cancer risk: systematic review and meta-regression analysis. Lancet. 2004; 363:1346–1353. [PubMed: 15110491]

Sakko AJ, Ricciardelli C, Mayne K, Suwiwat S, LeBaron RG, Marshall VR, et al. Modulation of prostate cancer cell attachment to matrix by versican. Cancer Res. 2003; 63:4786–4791. [PubMed: 12941795]

Schmalhofer O, Brabletz S, Brabletz T. E-cadherin, beta-catenin, and ZEB1 in malignant progression of cancer. Cancer Metastasis Rev. 2009; 28:151–166. [PubMed: 19153669]

Schneider R, Grosschedl R. Dynamics and interplay of nuclear architecture, genome organization, and gene expression. Genes Dev. 2007; 21:3027–3043. [PubMed: 18056419]

Smith SC, Theodorescu D. Learning therapeutic lessons from metastasis suppressor proteins. Nat Rev Cancer. 2009; 9:253–264. [PubMed: 19242414]

Song Y, Maul RS, Gerbin CS, Chang DD. Inhibition of anchorage-independent growth of transformed NIH3T3 cells by epithelial protein lost in neoplasm (EPLIN) requires localization of EPLIN to actin cytoskeleton. Mol Biol Cell. 2002; 13:1408–1416. [PubMed: 11950948]

Sung SY, Hsieh CL, Law A, Zhau HE, Pathak S, Multani AS, et al. Coevolution of prostate cancer and bone stroma in three-dimensional coculture: implications for cancer growth and metastasis. Cancer Res. 2008; 68:9996–10003. [PubMed: 19047182]

Thiery JP, Acloque H, Huang RY, Nieto MA. Epithelial-mesenchymal transitions in development and disease. Cell. 2009; 139:871–890. [PubMed: 19945376]

Thiolloy S, Rinker-Schaeffer CW. Thinking outside the box: Using metastasis suppressors as molecular tools. Semin Cancer Biol. 2010

Tusher VG, Tibshirani R, Chu G. Significance analysis of microarrays applied to the ionizing radiation response. Proc Natl Acad Sci U S A. 2001; 98:5116–5121. [PubMed: 11309499]

Varambally S, Yu J, Laxman B, Rhodes DR, Mehra R, Tomlins SA, et al. Integrative genomic and proteomic analysis of prostate cancer reveals signatures of metastatic progression. Cancer Cell. 2005; 8:393–406. [PubMed: 16286247]

Wei J, Xu G, Wu M, Zhang Y, Li Q, Liu P, et al. Overexpression of vimentin contributes to prostate cancer invasion and metastasis via src regulation. Anticancer Res. 2008; 28:327–334. [PubMed: 18383865]

Wellner U, Schubert J, Burk UC, Schmalhofer O, Zhu F, Sonntag A, et al. The EMT-activator ZEB1 promotes tumorigenicity by repressing stemness-inhibiting microRNAs. Nat Cell Biol. 2009; 11:1487–1495. [PubMed: 19935649]

Willipinski-Stapelfeldt B, Riethdorf S, Assmann V, Woelfle U, Rau T, Sauter G, et al. Changes in cytoskeletal protein composition indicative of an epithelial-mesenchymal transition in human micrometastatic and primary breast carcinoma cells. Clin Cancer Res. 2005; 11:8006–8014. [PubMed: 16299229]

Wong SY, Haack H, Kissil JL, Barry M, Bronson RT, Shen SS, et al. Protein 4.1B suppresses prostate cancer progression and metastasis. Proc Natl Acad Sci U S A. 2007; 104:12784–12789. [PubMed: 17640904]

Wu D, Zhau HE, Huang WC, Iqbal S, Habib FK, Sartor O, et al. cAMP-responsive element-binding protein regulates vascular endothelial growth factor expression: implication in human prostate cancer bone metastasis. Oncogene. 2007; 26:5070–5077. [PubMed: 17310988]

Xu J, Wang R, Xie ZH, Odero-Marah V, Pathak S, Multani A, et al. Prostate cancer metastasis: role of the host microenvironment in promoting epithelial to mesenchymal transition and increased bone and adrenal gland metastasis. Prostate. 2006; 66:1664–1673. [PubMed: 16902972]

Yamazaki D, Kurisu S, Takenawa T. Regulation of cancer cell motility through actin reorganization. Cancer Sci. 2005; 96:379–386. [PubMed: 16053508]

Yilmaz M, Christofori G. EMT, the cytoskeleton, and cancer cell invasion. Cancer Metastasis Rev. 2009; 28:15–33. [PubMed: 19169796]

Yilmaz M, Christofori G. Mechanisms of motility in metastasizing cells. Mol Cancer Res. 2010; 8:629–642. [PubMed: 20460404]

Yu YP, Landsittel D, Jing L, Nelson J, Ren B, Liu L, et al. Gene expression alterations in prostate cancer predicting tumor aggression and preceding development of malignancy. J Clin Oncol. 2004; 22:2790–2799. [PubMed: 15254046]

Zhang S, Zhau HE, Osunkoya AO, Iqbal S, Yang X, Fan S, et al. Vascular endothelial growth factor regulates myeloid cell leukemia-1 expression through neuropilin-1-dependent activation of c-MET signaling in human prostate cancer cells. Mol Cancer. 2010; 9:9. [PubMed: 20085644]

Zhau HE, Odero-Marah V, Lue HW, Nomura T, Wang R, Chu G, et al. Epithelial to mesenchymal transition (EMT) in human prostate cancer: lessons learned from ARCaP model. Clin Exp Metastasis. 2008; 25:601–610. [PubMed: 18535913]

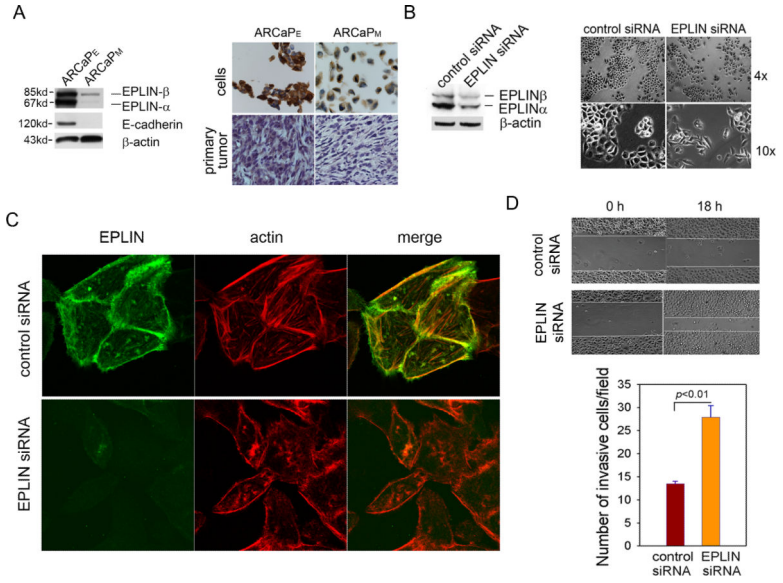

Figure 1. EPLIN depletion promotes EMT and enhances *in vitro* migration and invasion

(A) Expression of EPLIN in ARCaP cells and xenograft tumors. Left panel: Western blot analysis of EPLIN and E-cadherin in $ARCaP_E$ and $ARCaP_M$ cells. Right panel: immunocytochemical and immunohistochemical staining of EPLIN expression in ARCaP cells (top) and subcutaneous tumor tissues (bottom). (B) Left panel: effects of EPLIN siRNA transfection (72 h) on EPLIN protein expression in $ARCaP_E$ cells. Right panel: effects of EPLIN siRNA transfection on the morphology of $ARCaP_E$ cells. (C) Immunofluorescence staining of EPLIN and phalloidin staining of F-actin in $ARCaP_E$ cells transfected with EPLIN or control siRNA for 72 h. (D) Effects of EPLIN siRNA transfection on the *in vitro* migration (left panel) and invasion (right panel) in $ARCaP_E$ cells. The assays were performed at 18 h following cell seeding. Bars denote the standard error (n=3).

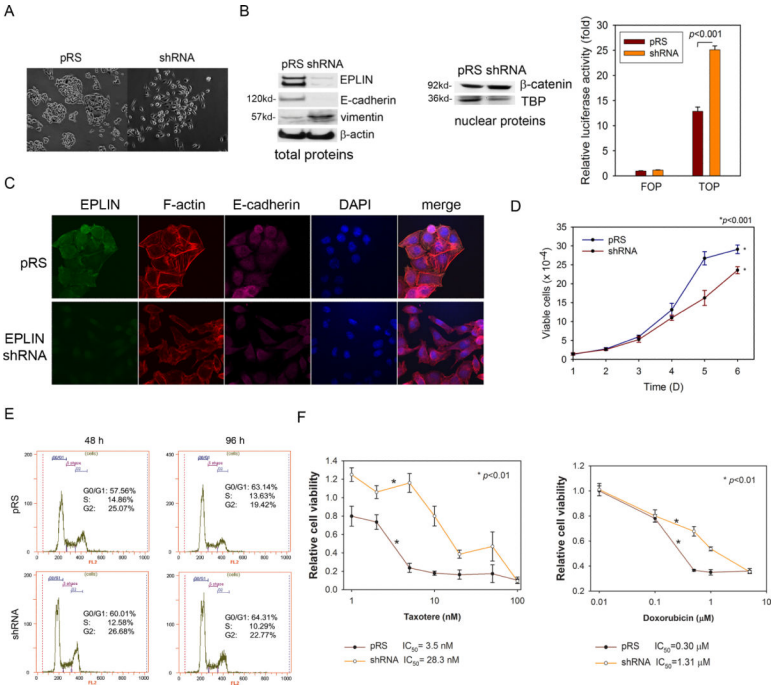

Figure 2. EPLIN depletion inhibits E-cadherin expression, activates β-catenin signaling, suppresses proliferation and enhances chemoresistance

(A) Comparison of the morphology of $ARCaP_E$ cells stably expressing EPLIN shRNA ($ARCaP_E$-shRNA, clone#102) or control pRS ($ARCaP_E$-pRS) constructs. (B) Effects of EPLIN depletion on the expression of EMT markers (E-cadherin and vimentin, left panel), nuclear translocation of β-catenin (central panel), and TCF promoter activity (right panel) in $ARCaP_E$ cells. Bars denote the standard error (n=3). (C) Effects of EPLIN depletion on the actin cytoskeleton and membrane E-cadherin expression in $ARCaP_E$ cells. (D) Proliferation of $ARCaP_E$-shRNA cells and control cells. Bars denote the standard error (n=6). (E) Cell cycle profiles of $ARCaP_E$-shRNA and control cells at 48 h and 96 h following cell seeding. *Y*-axis: cell numbers. (F) Effects of EPLIN depletion on the chemoresistance to docetaxel and Doxorubicin in $ARCaP_E$ cells, as analyzed by MTT assays.

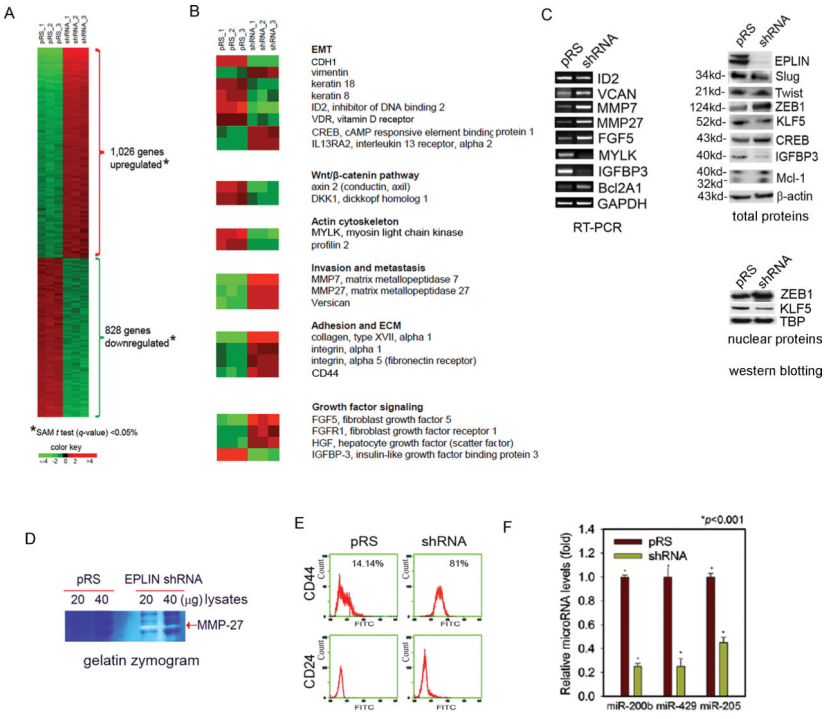

Figure 3. EPLIN downregulation activates multiple pro-EMT genes

(A) Microarray analysis of gene expression profile in $ARCaP_E$-pRS and $ARCaP_E$-shRNA cells. (B) Selected genes affected by EPLIN depletion in $ARCaP_E$ cells. (C) Validation of several putative EPLIN target genes. Left panel: RT-PCR analysis of the effects of EPLIN depletion on the expression of several selected genes in $ARCaP_E$ cells. Right panel: Western blot analysis of the effects of EPLIN depletion on protein expression in the total lysates (top) and nuclear extracts (bottom) in $ARCaP_E$ cells. (D) Effects of EPLIN depletion on the expression of active MMP-27 in $ARCaP_E$ cells, as analyzed by gelatin zymogram. (E) Effects of EPLIN depletion on the membrane expression of CD44 in $ARCaP_E$ cells, as analyzed by fluorescence-activated Cell Sorting (FACS). *Y*-axis: cell numbers. (F) Real-time qPCR analysis of the effects of EPLIN depletion on the expression of miR-200b, miR-429 and miR-205 in $ARCaP_E$ cells.

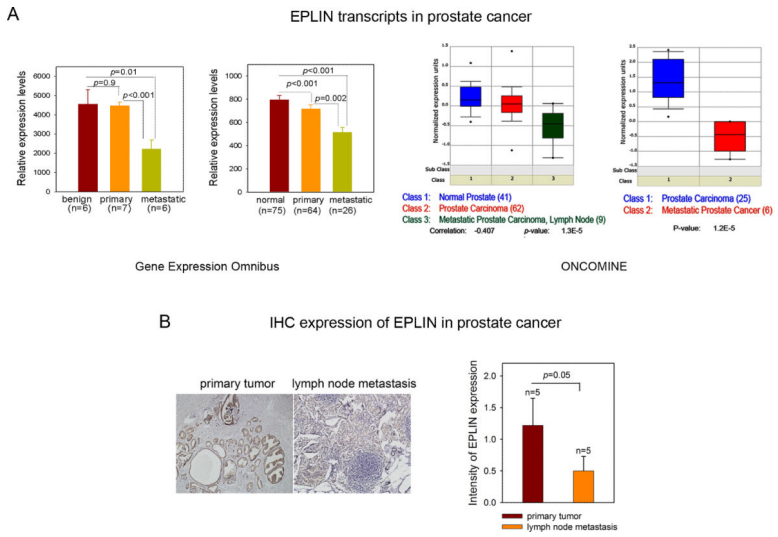

Figure 4. EPLIN downregulation correlates with PCa lymph node metastasis

(A) Microarray data-mining of EPLIN transcript expression in primary and metastatic PCa. (B) IHC expression of EPLIN were examined in matched pairs of specimens from primary and lymph node metastatic PCa and compared for the statistical significance. Bars denote the standard error.

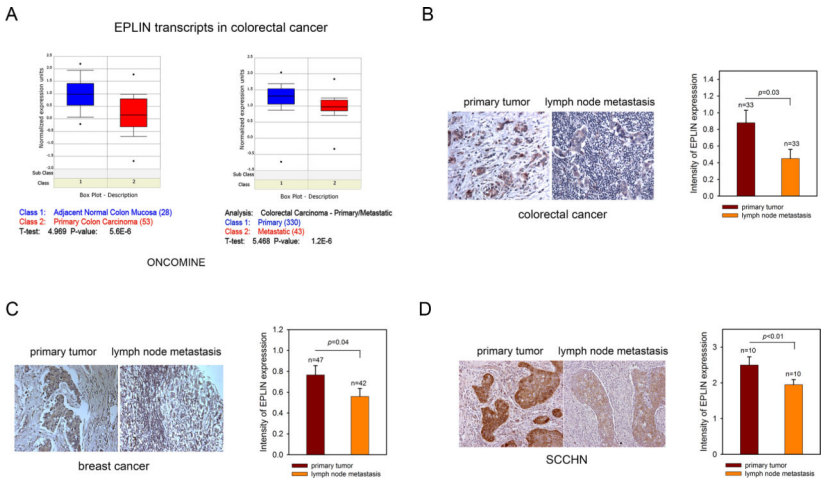

Figure 5. EPLIN downregulation correlates with clinical lymph node metastasis in breast cancer, colorectal cancer and SCCHN

(A) Microarray data-mining of EPLIN transcript expression in primary and metastatic colorectal cancer. IHC expression of EPLIN were examined in matched pairs of tumor tissues specimens or TMAs and compared for the statistical significance in human colorectal cancer (B), breast cancer (C) and SCCHN (D). Bars denote the standard error.

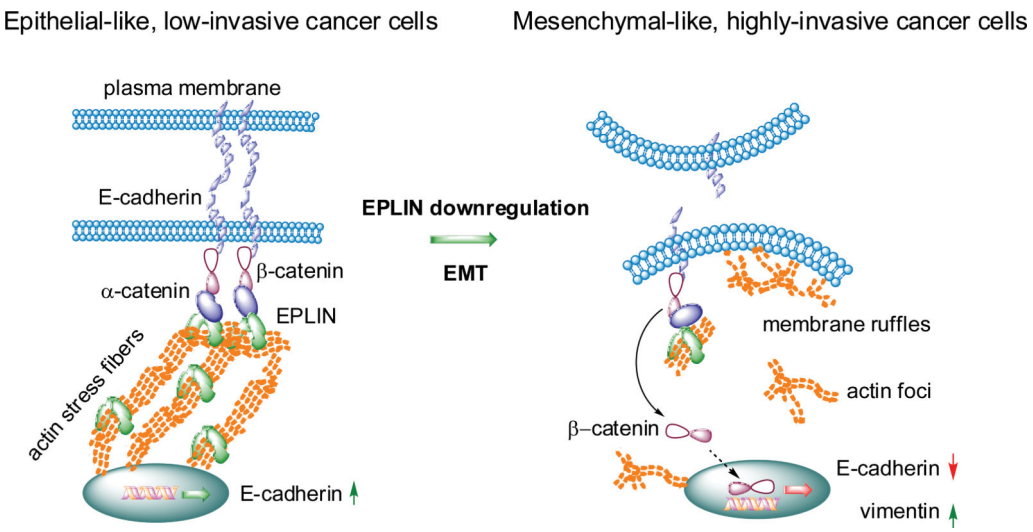

Figure 6. A proposed model for the role of EPLIN in PCa EMT and metastasis

Epithelial-like, low-invasive cancer cells (such as $ARCaP_E$) are joined by adherens junctions mediated by E-cadherin. The cytoplasmic tails of cadherin dimers bind to intracellular β-catenin. α-catenin binds to β-catenin, and is linked with actin filaments *via* EPLIN. EPLIN downregulation results in the disintegration of adherens junctions, remodeling of the actin cytoskeleton and activation of β-catenin signaling, which may further lead to the activation of multiple pro-EMT and -metastasis genes. These morphological, molecular and cellular alterations may significantly contribute to EMT and increase the invasiveness of PCa cells.

Table 1

Quantitative proteomic analysis of protein expression in PCa cells

A. Report statistics of cICAT proteomics in $ARCaP_E$ and $ARCaP_M$ cells (2338 total spectra):					
Confidence (ProtScore) Cutoff	**Proteins Identified**	**Proteins before Grouping**	**Distinct Peptides**	**Spectra Identified**	**% of Total Spectra**
>99 (2.0)	160	804	798	1823	78.0
>95 (1.3)	343	1607	998	2178	93.2
>66 (0.47)	458	2064	1121	2319	99.2
Report Parameters: ProtScore threshold: 1.20; Show competitor proteins within ProtScore: 1.20; Software version: 1.0.2					

B. Proteins significantly altered in $ARCaP_E$ and ARCaPM cells		
Accession	**Protein**	**Fold Change** *†
Increased expression		
IPI00103355.1	Cytochrome P450 2F1	2.0225
IPI00418471.5	Vimentin	1.8046
IPI00418169.3	annexin A2 isoform 1	1.6253
IPI00220327.2	Keratin, type II cytoskeletal 1	1.5625
IPI00556038.2	CDNA FLJ20203 fis, clone COLF1334	1.4706
IPI00014537.3	Isoform 1 of Calumenin precursor	1.4183
IPI00013991.1	Isoform 1 of Tropomyosin beta chain	1.3734
IPI00550766.1	NNP-1 protein	1.3666
IPI00376215.2	Isoform 2 of DNA-dependent protein kinase catalytic subunit	1.3567
IPI00414264.2	sorcin isoform b	1.3444
IPI00171152.1	abhydrolase domain containing 11 isoform 2	1.3379
IPI00217468.2	Histone H1.5	1.315
IPI00018349.5	DNA replication licensing factor MCM4	1.3106
IPI00183695.8	Protein S100-A10	1.3048
IPI00398585.5	Isoform 2 of Hook homolog 2	1.3004
IPI00025491.1	Eukaryotic initiation factor 4A-I	1.2984
IPI00741886.2	PREDICTED: similar to HLA class II histocompatibility antigen, DRB1-1 beta chain precursor	1.2858
IPI00157351.3	OTTHUMP00000045700	1.2857

B. Proteins significantly altered in ARCaP$_E$ and ARCaPM cells		
Accession	**Protein**	**Fold Change**[*†]
IPI00009901.1	Nuclear transport factor 2	1.2782
IPI00003362.2	Hypothetical protein	1.2753
IPI00797917.1	26 kDa protein	1.263
IPI00220766.3	Lactoylglutathione lyase	1.2527
IPI00025512.2	Heat-shock protein beta-1	1.2498
IPI00023006.1	Actin, alpha cardiac muscle 1	1.2437
IPI00478970.1	Hypothetical protein MGC16372	1.2418
IPI00029048.2	Tubulin--tyrosine ligase-like protein 12	1.2403
IPI00029744.1	Single-stranded DNA-binding protein, mitochondrial precursor	1.2339
IPI00009904.1	Protein disulfide-isomerase A4 precursor	1.23
IPI00220301.4	Peroxiredoxin-6	1.2163
IPI00791157.1	16 kDa protein	1.2157
IPI00216691.4	Profilin-1	1.2029
Decreased expression		
IPI00019205.1	Protein C14orf4	0.1028
IPI00218130.2	Glycogen phosphorylase, muscle form	0.2191
IPI00008918.1	Isoform Beta of LIM domain and actin-binding protein 1; EPLIN-Beta	0.2218
IPI00384897.3	PREDICTED: similar to Mucin-5B precursor	0.2543
IPI00032313.1	Protein S100-A4	0.5059
IPI00003110.2	Growth factor independence-1B	0.5779
IPI00744835.1	Isoform Sap-mu-9 of Proactivator polypeptide precursor	0.5838
IPI00291809.4	PREDICTED: similar to ankyrin repeat domain 24	0.6056
IPI00219757.12	Glutathione S-transferase P	0.6144
IPI00218914.4	Retinal dehydrogenase 1	0.6313
IPI00030154.1	Proteasome activator complex subunit 1	0.6323
IPI00789310.1	37 kDa protein	0.6374
IPI00797038.1	mitochondrial phosphoenolpyruvate carboxykinase 2 isoform 1 precursor	0.6586
IPI00746205.1	proteasome activator subunit 2	0.6848
IPI00747047.1	Treacle major isoform	0.6892

B. Proteins significantly altered in ARCaP$_E$ and ARCaPM cells		
Accession	**Protein**	**Fold Change**[*†]
IPI00418790.2	echinoderm microtubule associated protein like 5	0.694
IPI00514204.3	Lamin A/C	0.7052
IPI00215911.2	DNA-(apurinic or apyrimidinic site) lyase	0.7139
IPI00017297.1	Matrin-3	0.7177
IPI00784347.1	Keratin, type I cytoskeletal 18	0.7218
IPI00472448.1	Isoform 1 of HLA class I histocompatibility antigen, A-11 alpha chain precursor	0.7227
IPI00554648.2	Keratin, type II cytoskeletal 8	0.7258
IPI00018755.1	High mobility group protein 1-like 10	0.726
IPI00017510.3	Cytochrome c oxidase subunit 2	0.7319
IPI00007752.1	Tubulin beta-2C chain	0.7489
IPI00794319.1	9 kDa protein	0.7515
IPI00337544.7	phosphodiesterase 4D interacting protein isoform 5	0.7561
IPI00303476.1	ATP synthase subunit beta, mitochondrial precursor	0.7733
IPI00292387.5	Isoform Alpha of Nucleolar phosphoprotein p130	0.7842
IPI00024920.1	ATP synthase delta chain, mitochondrial precursor	0.7913
IPI00550020.2	Parathymosin	0.7927
IPI00647118.1	14 kDa protein	0.8043
IPI00007765.5	Stress-70 protein, mitochondrial precursor	0.8068
IPI00549248.4	Isoform 1 of Nucleophosmin	0.8094
IPI00020984.1	Calnexin precursor	0.8123
IPI00000874.1	Peroxiredoxin-1	0.8196
IPI00025086.3	Cytochrome c oxidase subunit 5A, mitochondrial precursor	0.8253
IPI00008527.3	60S acidic ribosomal protein P1	0.8263
IPI00301311.1	Isoform 2 of Protein SET	0.8291
IPI00791301.1	46 kDa protein	0.8342
IPI00218200.7	B-cell receptor-associated protein 31	0.8344
IPI00075248.10	Calmodulin	0.8388
IPI00479694.1	PREDICTED: similar to 40S ribosomal protein S26	0.8427
IPI00002459.4	annexin VI isoform 2	0.8438

B. Proteins significantly altered in ARCaP$_E$ and ARCaPM cells		
Accession	**Protein**	**Fold Change*†**
IPI00000816.1	14-3-3 protein epsilon	0.8477

* Ratio: relative protein expression in ARCaP$_M$ *vs.* ARCaP$_E$ cells

† $p<0.05$